Design of a Non-cooperative Target Capture Mechanism

WANG Chen, NIE Hong, CHEN Jinbao, PAN Zhengwei*

State Key Laboratory of Mechanics and Control of Mechanical Structures, Nanjing University of Aeronautics and Astronautics, Nanjing 210016, P.R. China

(Received 11 June 2017; revised 22 August 2017; accepted 14 September 2017)

Abstract: A passive compliant non-cooperative target capture mechanism is designed to maintain the non-cooperative target on-orbit. When the relative position between capture mechanism and satellite is confirmed, a pair of four-bar linkages lock the docking ring, which is used for connecting the satellite and the rocket. The mathematical model of capture mechanism and capture space is built by the Denavit-Hartenberg(D-H) method, and the torque of each joint is analyzed by the Lagrange dynamic equation. Besides, the capture condition and the torque of every joint under different capture conditions are analyzed by simulation in MSC. Adams. The results indicate that the mechanism can capture the non-cooperative target satellite in a wide range. During the process of capture, the passive compliant mechanism at the bottom can increase capture space, thereby reducing the difficulty and enhance stability of the capture.

Key words: non-cooperative target; passive compliance; capture mechanism; kinematics analysis; dynamics analysis

CLC number: V423.9 **Document code**: **Article ID**: 1005-1120(2019)01-0146-08

0 Introduction

With the continuous development of space mission, the on-orbit capture technology has become a hot research topic in the field of astronautics [1]. So far, the capture of cooperative target has been a mature technology and successfully applied in the field of on-orbit service. However, the capture of non-cooperative targets has not been verified in space. In view of the importance of non-cooperative target capture in space, all the powerful countries focus on related researches [2]. German Aerospace Center has carried out Technology Satellite for Demonstration and Verification of Space Systems/Deutsche Orbital Servicing (TECSAS/DEOS) Mission, which focuses on unmanned orbital repairing and assembly [3]. The American Front End Robotics Enabling Near-term Demonstration (FREND) plans to take advantage of the docking ring which is used for connecting the satellite and the rocket as the interface to capture the target satellite and modify its orbit[4-7]. In China, Wang [8] designed a non-cooperative target capture mechanism to capture the apogee engine nozzle of satellite, based on the principle of envelope trapping. The capture is operated by three uniformly distributed manipulators and the capture mechanisms on them. Li[9-10] optimized the capture mechanism and proposed a long stroke and miniaturized capture mechanism for apogee engine nozzle.

The size and mass of present capture mechanisms for apogee engine nozzle are larger, which increase the difficulty and cost of launch. Beyond that, they cannot accommodate or correct the deviation of initial docking condition. A capture mechanism is proposed in this paper, which is lighter and smaller. Its target is the docking ring, which is used for connecting the satellite and the rocket. The docking ring has better structure strength and wider applications than apogee engine nozzle. Additionally, the passive compliant mechanism of capture mechanism can increase the working space. Then the capture mechanism can capture the target satellite with large tolerance.

According to the non-cooperative target cap-

*Corresponding author, E-mail address: hnie@nuaa.edu.cn.

How to cite this article: WANG Chen, NIE Hong, CHEN Jinbao, et al. Design of a Non-cooperative Target Capture Mechanism[J]. Transactions of Nanjing University of Aeronautics and Astronautics, 2019,36(1):146-153.
http://dx.doi.org/10.16356/j.1005-1120.2019.01.014

ture mechanism, a kinematic model is established to analyze the capture space. Then the relationship between the passive compliant mechanism at the bottom and the capture performance of the mechanism is obtained. The dynamic model is established by the Lagrange dynamic equation and the driving torque of every joint of capture mechanism is solved. The capture mechanism is verified under different conditions by system dynamics simulation. The results indicate that the mechanism can capture the target satellite with large tolerance.

1 Working Principle and Design of the Capture Mechanism

The capture target of capture mechanism is the docking ring, which is used for connecting the satellite and the rocket. The docking ring an international standard interface and widely used in various spacecraft, whose structure and size are shown in Fig. 1. The outer diameter is 1 194 mm, inner diameter is 1 133 mm, entire height is 320 mm and the step surface has a dimension of 5.72 mm. The capture method proposed in this paper employs three capture mechanisms, which are uniformly distributed relative to the axis of satellite docking ring. They capture the target docking ring one after another, and then the entire capture process is completed. The capture result is shown in Fig. 2. The result of single physical mechanism captured part of docking ring is shown in Fig. 3.

Take one of the capture mechanisms as an example, as shown in Fig. 4. The passive compliant mechanism at bottom can provide the passive compliance of horizontal slide and vertical rotation, then

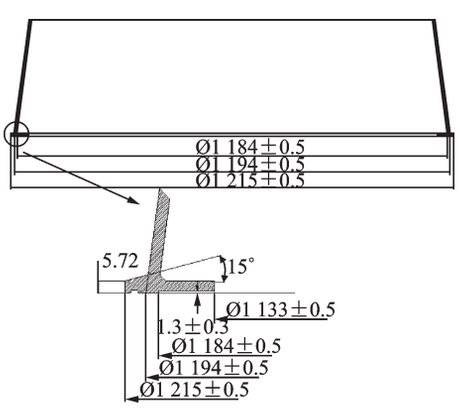

Fig. 1 Docking ring for Ø1 194A (satellite part)

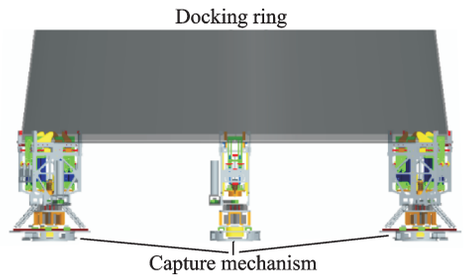

Fig. 2 Three capture mechanisms captured the satellite

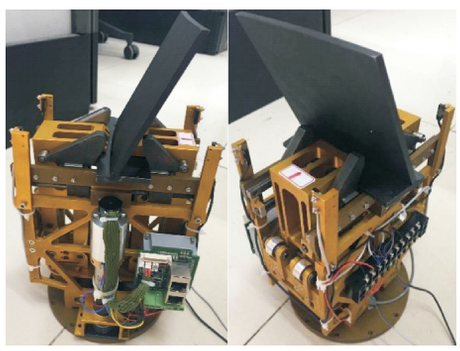

Fig. 3 Single physical capture mechanism captured part of docking ring

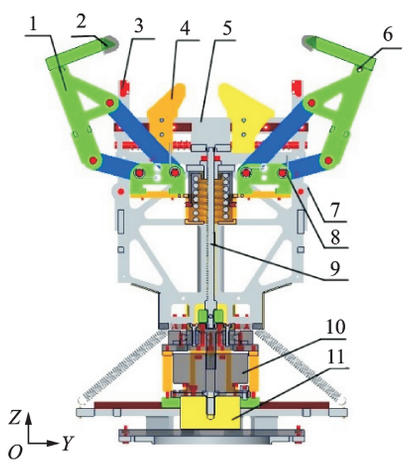

1—Four-bar linkages capture claw; 2—Rubber gloves;
3—Photoelectric sensor; 4—Horizontal locking mechanism;
5—Supporting platform; 6—Pressing bar; 7—Roller;
8—Torsion spring; 9—Screw; 10—Rotation brake; 11—Slide brake

Fig. 4 Profile of capture mechanism

the capture mechanism can accommodate position tolerance and angle tolerance. Detailed technical indexes are shown in Table 1.

Combining with Fig. 4, the entire capture process is introduced as follows: (1) The capture mechanism is installed at the end of the manipulator. The motor drives four-bar linkages capture mechanism to move upwards along the screw, and its mechanical limit is lifted during the upward movement. Then it deploys by torsion spring. (2) The manipu-

Table 1 Technical indexes of capture mechanism

Passive compliance range	Horizontal slide/mm	115
	Vertical rotation/(°)	360
Capture tolerance	Position tolerance (Three axes)/mm	±50
	Angle tolerance (Three axes)/(°)	±10
Locking load	X, Y, Z/(N·m)	≥200

lator which is equipped with capture mechanism moves along the Z^+ axis, subsequently the 1. capture claws are stuck into the satellite docking ring. (3) When the photo electric sensor detects the docking ring, the motor drives the four-bar linkages capture claws to move downwards along the screw. At the same time, the rollers on both sides drive four-bar linkages capture claws to close, and the pressing bars on the capture claws drive horizontal locking mechanism to move along the Y axis. Both four-bar linkages capture claws and horizontal locking mechanism surround the docking ring gradually and complete the capture. (4) The bottom of docking ring stops on the supporting platform, and the capture claws press on the 5.72 mm step surface. Meanwhile, the horizontal locking mechanism locks the inner and outer surfaces of docking ring along the Y axis. (5) After the capture and locking complete, both rotation and slide brake apply. The kinematic diagram of capture mechanism is shown in Fig.5[11]. The entire capture process is shown in Fig.6.

2 Kinematic Analysis of Capture Mechanism

Since two four-bar linkages capture claws of the capture mechanism are symmetrically distributed, the one in the left is taken as an example. As shown in Fig.7, its coordinate systems are established and working space is analyzed by Denavit-Hartenberg (D-H) method. Its detailed parameters are shown in Table 2[12].

The transformation matrix from coordinate system $\{i-1\}$ to the coordinate system $\{i\}$ is shown as follow

$$ {}^0_6T = {}^0_1T\,{}^1_2T\,{}^2_3T\,{}^3_4T\,{}^4_5T\,{}^5_6T \tag{1} $$

If the passive compliant mechanism is not considered, its transformation matrix is shown as follows

$$ {}^2_6T = {}^2_3T\,{}^3_4T\,{}^4_5T\,{}^5_6T \tag{2} $$

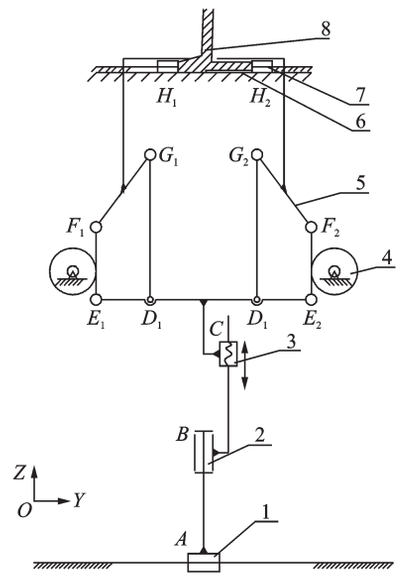

1—Liner guide; 2—Turntable bearing; 3—Screw; 4—Roller; 5—Four-bar linkages capture claw; 6—Supporting platform; 7—Horizontal locking mechanism; 8—Docking ring

Fig.5 Kinematic diagram of capture mechanism

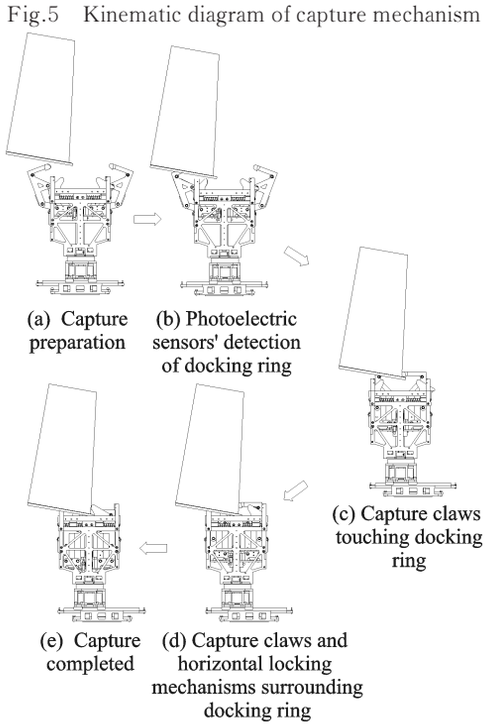

Fig.6 Target satellite docking capture process

The detailed parameters of four-bar linkages capture claw are: $S_1 \in [-57, 57]$ mm, $\theta_2 \in [0°, 180°]$, $L_1 = 56$ mm, $L_2 \in [0°, 80°]$ mm, $L_3 = 19$ mm, $L_4 = 40$ mm, $\theta_4 \in [0°, 75°]$, $\theta_5 \in [0°, 54°]$, $L_{5y} = 45$ mm, $L_{5z} = 84$ mm.

The capture spaces in two cases are drawn by Matlab, as shown in Figs.8, 9, both their coordinate directions are same as Fig.7.

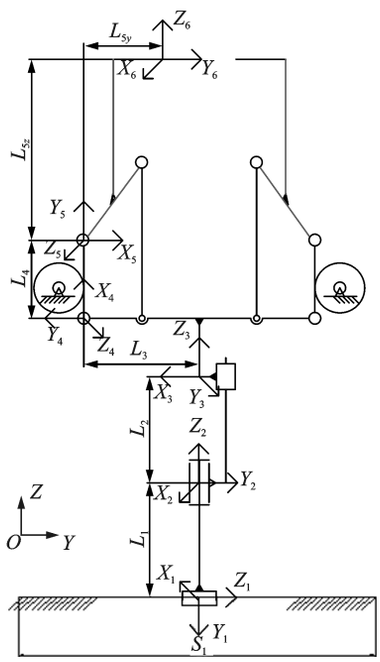

Fig.7 Coordinate systems for docking capture mechanism

Table 2 Linkage parameters for capture mechanism

i	1	2	3	4	5	6
α_{i-1}/(°)	−90	−90	0	−90	0	−90
a_{i-1}/mm	0	0	0	L_3	L_4	L_{5y}
d_i/mm	S_1	L_1	L_2	0	0	L_{5z}
θ_i/(°)	0	θ_2	−90	θ_4-90	θ_5-90	−90

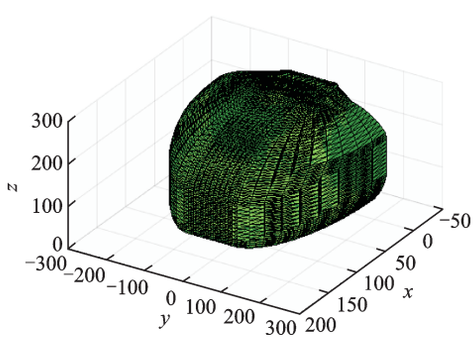

Fig.8 Capture space of left four bar-linkages capture claw

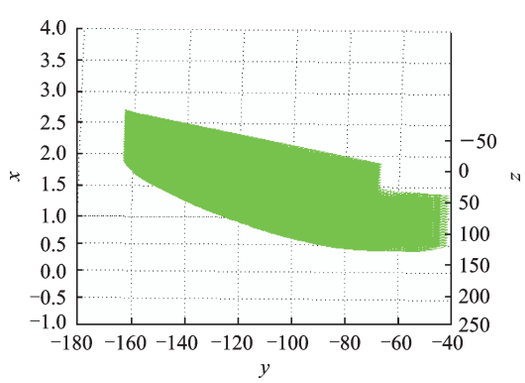

Fig.9 Capture space of left four bar-linkages capture claw without passive compliant mechanism

By comparing Fig.8 with Fig.9, it can be found that the passive compliant mechanism at bottom greatly increases the working space of capture mechanism, especially on the X axis. The space along the X axis is close to $[-50,150]$ mm, the Y axis is close to $[-200, 200]$ mm, and the Z axis is close to $[0,250]$ mm. It is proved that the passive compliant mechanism at bottom can significantly improve the capture performance of capture mechanism.

3 Dynamics Analysis of Capture Mechanism

The dynamics equation of the left four-bar linkages capture claw is obtained by the Lagrange dynamics equation.

$$\boldsymbol{\tau}=\frac{\mathrm{d}}{\mathrm{d}t}\frac{\partial L}{\partial\dot{\boldsymbol{\theta}}}-\frac{\partial L}{\partial\boldsymbol{\theta}} \tag{3}$$

In the Eq.(3), $\boldsymbol{\tau}=[\tau_1\ \tau_2]^{\mathrm{T}}$ is the generalized torque of the joint, $\boldsymbol{\theta}=[\theta_1\theta_2]^{\mathrm{T}}$ is the angular acceleration of the joint, and L is the Lagrange function shown as

$$L(\boldsymbol{\theta},\dot{\boldsymbol{\theta}})=K(\boldsymbol{\theta},\dot{\boldsymbol{\theta}})-U(\boldsymbol{\theta}) \tag{4}$$

where $U(\boldsymbol{\theta})$ is the sum of geopotential energy of system and $K(\boldsymbol{\theta},\ \dot{\boldsymbol{\theta}})$ the sum of kinetic energy of system [13].

The link BC and the upper claw are simplified as a link with uniformly-distributed mass, whose length is l_2 and centroid m_2 locates at the center of the link. θ_1 is chosen as the generalized coordinate. After simplification, the dynamics diagram of the four-bar linkages capture claw is shown in Fig.10[14-15].

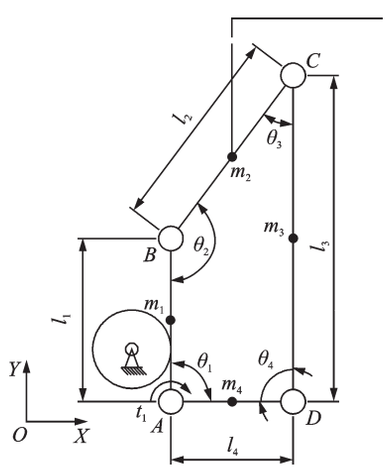

Fig.10 Dynamics of let capture claw before capture collision

The length of the link AB, BC and CD are l_1, l_2, and l_3, respectively. The kinetic energy of each link can be obtained.

$$K_1 = \frac{1}{2} m_1 \dot{\boldsymbol{P}}_{C_1}{}^{\mathrm{T}} \dot{\boldsymbol{P}}_{C_1} + \frac{1}{2} \boldsymbol{\omega}_1{}^{\mathrm{T}} \boldsymbol{I}_1 \boldsymbol{\omega}_1 = \frac{1}{6} m_1 l_1{}^2 \dot{\theta}_1^2 \tag{5}$$

$$K_2 = \frac{1}{2} m_2 \dot{\boldsymbol{P}}_{C_2}{}^{\mathrm{T}} \dot{\boldsymbol{P}}_{C_2} + \frac{1}{2} \boldsymbol{\omega}_2{}^{\mathrm{T}} \boldsymbol{I}_2 \boldsymbol{\omega}_2 = \left(\frac{1}{2} m_2 l_1{}^2 + \frac{1}{6} m_2 l_2{}^2 + \frac{1}{2} m_2 l_1 l_2 c\theta_2\right)\dot{\theta}_1{}^2 + \left(\frac{1}{3} m_2 l_2{}^2 + \frac{1}{2} m_2 l_1 l_2 c\theta_2\right)\dot{\theta}_1\dot{\theta}_2 + \frac{1}{6} m_2 l_2{}^2 \dot{\theta}_2{}^2 \tag{6}$$

$$K_3 = \frac{1}{2} m_3 \dot{\boldsymbol{P}}_{C_3}{}^{\mathrm{T}} \dot{\boldsymbol{P}}_{C_3} + \frac{1}{2} \boldsymbol{\omega}_3{}^{\mathrm{T}} \boldsymbol{I}_3 \boldsymbol{\omega}_3 = \left(\frac{1}{6} m_1 l_1{}^2 + \frac{1}{2} m_2 l_1{}^2 + \frac{1}{2} m_3 l_1{}^2 + \frac{1}{6} m_2 l_2{}^2 + \frac{1}{2} m_3 l_2{}^2 + \frac{1}{6} m_3 l_3{}^2 + \frac{1}{2} m_2 l_1 l_2 c\theta_2 + m_3 l_1 l_2 c\theta_2 + \frac{1}{2} m_3 l_1 l_3 c\theta_{23} + \frac{1}{2} m_3 l_2 l_3 c\theta_3\right)\dot{\theta}_1{}^2 + \left(\frac{1}{6} m_2 l_2{}^2 + \frac{1}{2} m_3 l_2{}^2 + \frac{1}{2} m_3 l_2 l_3 c\theta_3 + \frac{1}{6} m_3 l_3{}^2\right)\dot{\theta}_2{}^2 + \frac{1}{6} m_3 l_3{}^2 \dot{\theta}_3{}^2 + \left(\frac{1}{2} m_2 l_1 l_2 c\theta_2 + \frac{1}{3} m_2 l_2{}^2 + m_3 l_2{}^2 + \frac{1}{3} m_3 l_3{}^2 + m_3 l_1 l_2 c\theta_2 + \frac{1}{2} m_3 l_1 l_3 c\theta_{23} + m_3 l_2 l_3 c\theta_3\right)\dot{\theta}_1\dot{\theta}_2 + \left(\frac{1}{3} m_3 l_3{}^2 + \frac{1}{2} m_3 l_1 l_3 c\theta_{23} + \frac{1}{2} m_3 l_2 l_3 c\theta_3\right)\dot{\theta}_1\dot{\theta}_3 + \left(\frac{1}{3} m_3 l_3{}^2 + \frac{1}{2} m_3 l_2 l_3 c\theta_3\right)\dot{\theta}_2\dot{\theta}_3 \tag{7}$$

The total kinetic energy of the system is

$$K = K_1 + K_2 + K_3 \tag{8}$$

The capture mechanism is in the space without gravity, hence the geopotential energy is 0.

The torque of joint 1 can be obtained by Eq.(3)

$$\tau_1 = \frac{\mathrm{d}}{\mathrm{d}t}\left(\frac{\partial K}{\partial \dot{\theta}_1}\right) - \frac{\partial K}{\partial \theta_1} \tag{9}$$

The influence of the motion state of capture mechanism on driving torque IS obtained from the dynamic model, and the optimal capture angular velocity can be analyzed. When angular acceleration of θ_1 is 0, the relationship between the torque of joint 1, angle of θ_1 and angular velocity of θ_1 is shown in Fig.11. The torque of θ_1 increases with the increase of its angle. It increases first and then decreases according to the change of its angular velocity. When angular velocity is 2.74 rad/s, the torque is the largest, i.e., 43.40 N·mm.

4 Simulation

The 3D model of capture mechanism and the docking ring are imported into Adams2014 and the corresponding constraints are established. The simulation begins with the initial state that, at this moment, the target satellite docking ring has triggered the photoelectric sensor on capture mechanism, and their relative positions are confirmed. In addition, they are relatively static, and both the relative velocity and relative angular velocity are zero.

The coordinates on both centroid of the target satellite docking ring and centroid of capture mechanism supporting platform are built, as shown in Fig.12.

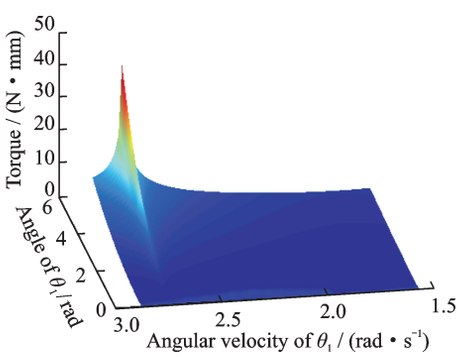

Fig.11 Relationship between the torque of joint 1, angle of θ_1 and angular velocity of θ_1

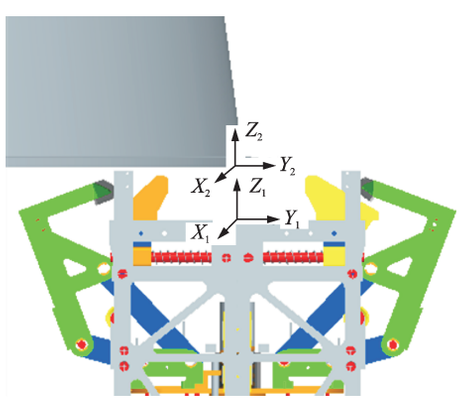

Fig.12 Centroid coordinates of target satellite docking ring and capture mechanism supporting platform

The "Measures" between two coordinates are built to measure the relative distance between them. The result is shown in Fig.13. It illustrates that the supporting platform of capture mechanism approaches the docking ring and the four-bar linkages capture claws get close gradually. Then the capture claw contacts the docking ring at about 1.37 s and the attitude of capture mechanism is adjusted by the passive compliant mechanism at bottom. Therefore, the curve is horizontal in a short time and has a slight rise, soon afterwards it goes down more steeply due to the attitude of capture mechanism changed. Then, the four-bar linkages capture claws continue to close gradually. At 5.22 s, the two capture claws press on the step surface of docking ring, thus the relative speed between them increases. The distance between them becomes 0 at 6.75 s and the entire capture process is accomplished. During the capture process, the torques of left four-bar linkages capture claw are shown in Fig.14. The capture claw contacts docking ring from 1.37 s to 1.78 s. During this period, the roller pushes link 1 to drive the four link mechanism close, and the docking ring is captured gradually. The torque of joint 1 is the largest and its peak is 176 N·mm. After four-bar linkages capture claws get closed, capture mechanism moves upwards along the Z axis and docking ring stops on the supporting platform, and the torque curve of every joint keeps stable basically.

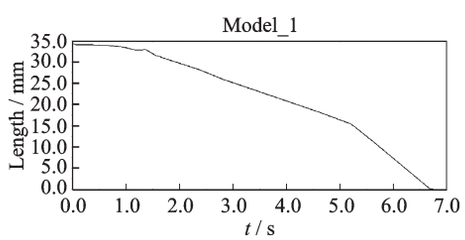

Fig.13 Relative distance between target satellite docking ring barycenter and capture mechanism supporting platform barycenter

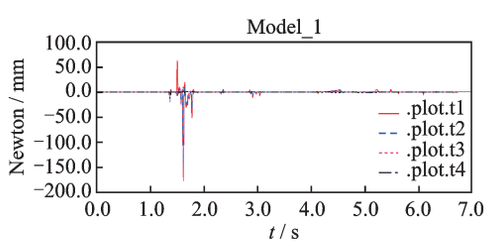

Fig. 14 Torque at left four bar-linkages capture claw joints during capture process

According to the technical indexes in Table 1, another simulation example under an extreme condition is analyzed to verify the performance of the capture mechanism. It is performed at the circumstance that the docking ring moves 50 mm along the $-Y$ axis and rotates 10° around the X axis. The results are shown in Figs.15, 16. As shown in Fig.15, the supporting platform of capture mechanism approaches the docking ring and the four-bar linkages capture claws get close gradually.

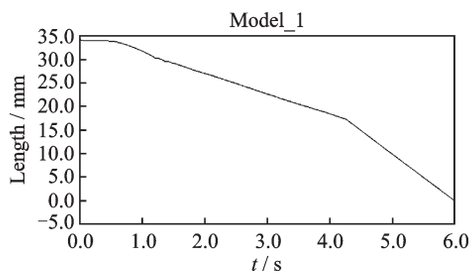

Fig. 15 Relative distance between target satellite docking ring barycenter and capture mechanism supporting platform barycenter after docking ring moves 50 mm along $-Y$ and rotates 10° along X clockwise

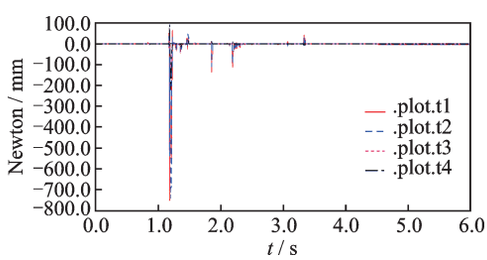

Fig.16 Torque at left four-bar linkages capture claw joints during capture process after docking ring moves 50 mm along $-Y$ and rotates 10° along X clockwise

Then, the capture claw contacts the docking ring at about 0.54 s, thus the relative speed between them increases. At 4.25 s, two capture claws press on the step surface of docking ring, thus the relative speed between them increases further. Finally, the distance between them becomes 0 at 5.96 s and the entire capture process is finished. It proves that the mechanism can still capture the target satellite docking ring successfully when it moves 50 mm along $-Y$ axis and rotates 10° around the X axis. As shown in Fig.16, the capture claw contacts docking ring from 1.17 s to 1.47 s. During this period the roller pushes

link 1 to drive the four-bar linkages mechanism close, and the docking ring is captured gradually. The torque of joint 1 is the largest and its peak is 739 N·mm. After four-bar linkages capture claws get closed, the torque of every joint keeps stable basically. At 1.86 s and 2.19 s, due to the position and angular deviation, the attitude of capture mechanism is adjusted twice by passive compliant mechanism at the bottom, leading to the peaks of 134 N·mm and 111 N·mm.

The simulation of two different circumstances prove that the capture mechanism with passive compliance can capture the target satellite docking ring successfully, with a position tolerance of ± 50 mm and an angle tolerance of $\pm 10°$ in any direction of X, Y, Z axes. However, they will increase the torques of joints during capture process and produce secondary peaks due to the attitude adjustment by passive compliant mechanism at the bottom. At the same time, the attitude adjustment causes a partial change in the relative trajectory between the docking ring and capture mechanism. Moreover, the tolerances cause a distance change between them, thus the capture time of two conditions is slightly different while the speeds of motor driving are same.

5 Conclusions

A non-cooperative target capture mechanism with passive compliance is proposed in this paper. It has the advantage of wide application range, large capture range, light weight and compact structure.

(1) The capture method for satellite docking ring can be applied to all kinds of spacecraft on-orbit with docking ring. The envelope size of entire capture mechanism is only 306 mm × 157 mm × 84 mm, and the weight is only 5.10 kg.

(2) The kinematic performance of the capture mechanism is analyzed by the D-H method, and its capture space is obtained. Then the drive torque of every joint is computed by Lagrange dynamics equation. It proves that the capture mechanism can accommodate large tolerance and has stable mechanical properties during capture process.

(3) Simulations are performed by MSC.Adams prove that the capture mechanism can capture target spacecraft stably, fast and reliably by automatic adjustment of the passive compliant mechanism, when both position deviation and angle deviation exist.

References

[1] WEI Wenshu, JING Wuxing, GAO Changsheng. Research automatic stability technology of spacecraft assembly with captured non-cooperative targets on orbit in chinese [J]. Acta aeronautica et Astronautica Sinica, 2013, 34(7):1520-1530.

[2] CAI Hongliang, GAO Yongming, BING Qijun, et al. The research status and key technology analysis of foreign non-cooperative target in space capture system [J]. Journal of the Academy of Equipment Command & Technology, 2010., 21(6):71-77.(in Chinese)

[3] MARTIN E, DUPUIS E, PIEDBOEUF J C, et al. The TECSAS mission from a Canadian Perspective [C]// Proceeding of the 8th International Symposium on Artificial Intelligence and Robotics and Automation in Space (i-SAIRAS). Munich, Germany: [s.n.], 2005.

[4] IANNOTTA B. Sumo wrestles satellites into new orbits [J]. Aerospace America, 2006, 44(2):26-30.

[5] DEBUS T J, DOUGHERTY S P. Overview and performance of the front-end robotics enabling near-term demonstration (FREND) robotic arm [C]// Proceedings of the 2009 AIAA Infotech@ Aerospace Conference. Seattle: AIAA, 2009:1-12.

[6] LIANG Bin, DU Xiaodong, LI Cheng, et al. Advances in space robot on-orbit servicing for non-cooperative spacecraft[J]. Robot, 20102, 34(2):242-256.(in Chinese)

[7] CHEN Luojing, HAO Jinhua, YUAN Chunzhu, et al. Key technology analysis and enlightenment of phoenix program in Chinese [J]. Spacecraft Engineering, 2013, 22(5):119-128.

[8] WANG Xiaoxue. Research on the docking and capture mechanism for the uncooperative target satellites[D]. Harbin: Harbin Institute of Technology, 2009. (in Chinese)

[9] LI Longqiu, LIU Weimin, CHEN Meng, et al. Design and analysis of non-cooperative target drag-and-drop docking mechanism in Chinese [J]. Chinese Space Science and Technology, 2015, 35(2):41-48.

[10] LI Longqiu, SHAO Guangbin, ZHOU Dekai, et al. Design and analysis of a long-stroke and miniaturized docking mechanism[J]. Manned Spaceflight, 2016, 22(6):758-765.

[11] ZHU Rupeng. Mechanical theory in Chinese [M].Beijing: Aviation Industry Press, 1998,8:9-12.
[12] CRAIG J J. Introduction to robotics in Chinese [M]. 3rd Edition. Beijing: Machinery Industry Press, 2006: 53-56 .(in Chinese)
[13] ZHANG Lixun, LU Dunmin, WANG Lan,et al. Dynamics analysis of five-bar cobot based on differential mechanism in Chinese [J]. Robot, 2004, 26(2):123-126.
[14] ZHANG Fan, HUANG Panfeng. Inertia parameter estimation for an noncooperative target captured by a space tethered system in Chinese [J]. Journal of Astronautics, 2015, 36(6):630-639.
[15] LIU Chuanshi. Study on the docking mechanism for uncooperative space target in Chinese [D]. Harbin: Harbin Institute of Technology, 2010.

Acknowledgement This work was supported by the National Natural Science Foundation of China (No.51675264).

Authors Mr. **WANG Chen** was born in 1992, a Ph.D candidate in Nanjing University of Aeronautics and Astronautics. His main research interest is flight vehicle design and dynamic analysis.

Prof. **NIE Hong** received the Ph.D. degrees in flight vehicle design from Nanjing University of Aeronautics and Astronautics, Nanjing, China, in 1990. His main research interest is the design of aircraft landing gear.

Prof. **CHEN Jinbao** received the Ph.D. degree in flight vehicle design from Nanjing University of Aeronautics and Astronautics, Nanjing, China, in 2007. His main research interest is the soft landing of lunar and space robot.

Mr. **PAN Zhengwei** is a master's candidate in Nanjing University of Aeronautics and Astronautics. His main research interest is flight vehicle design and dynamic analysis.

Author contributions Mr. **WANG Chen** contributed to design the mechanism, conduct the analysis and write the manuscript. Prof. **NIE Hong** and Prof. **CHEN Jinbao** contributed to write and polish the manuscript. Mr. **PAN Zhengwei** contributed to conduct the analysis. All authors commented on the manuscript draft and approved the submission.

Competing interests The authors declare no competing interests.

(Production Editor: Zhang Tong)